

IJP 02907

## Computer simulation of penetrant concentration-depth profiles in the stratum corneum

A.C. Watkinson<sup>a</sup>, A.L. Bunge<sup>b</sup>, J. Hadgraft<sup>a</sup> and A. Naik<sup>c</sup>

<sup>a</sup> *Welsh School of Pharmacy, University of Wales, PO Box 13, Cardiff CF1 3XF (UK)*, <sup>b</sup> *Chemical Engineering and Petroleum Refining Department, Colorado School of Mines, Golden, CO 80401 (USA)* and <sup>c</sup> *Department of Pharmacy and Pharmaceutical Chemistry, University of California, San Francisco, CA 94143 (USA)*

(Received 26 March 1992)

(Modified version received 8 April 1992)

(Accepted 8 April 1992)

**Key words:** Concentration/depth profiles; Stratum corneum; Penetration mechanism; Percutaneous penetration; Computer simulation; Oleic acid

---

### Summary

Approximate drug concentration-depth profiles in the stratum corneum (sc) have been achieved by computer simulation. In vivo data from the literature have been used to predict profiles for cases where the diffusion coefficient is not constant with depth. The effects of a penetration enhancer (oleic acid) on the profiles have been modelled using this technique. The results indicate that, except in the presence of an enhancer, the profiles are little altered by a position-dependent diffusion coefficient. It has been demonstrated that it is not necessarily correct to assume a logarithmic type fit to concentration-depth data collected from tape strip experiments.

---

### Introduction

The distribution of a drug in the skin is an important factor that must be considered when investigating its percutaneous absorption. A convenient way of representing this distribution is as a graph of the variation in drug concentration with depth into the stratum corneum (sc). The plot is usually normalised on both axes and a representative example is shown in Fig. 1a.

In many mathematical models for permeation through the sc the value of the diffusion coefficient

for the process is taken as constant. Evidence gained from attenuated total reflectance Fourier transform infrared (ATR-FTIR) studies (Guy et al. 1990) suggests that there is a decrease in the C-H stretch frequency ( $\nu$ ) associated with the lipid alkyl chains of the sc as the skin is penetrated. This decrease of approx.  $2\text{ cm}^{-1}$  after four tape strips (Guy et al. 1990) implies an increase in the ordering of the sc lipids with depth. If, as is often postulated (Mak et al., 1990; Potts and Francouer, 1990) penetration occurs predominantly via the intercellular lipid channels the above observation seems likely to imply a decrease in diffusion coefficient with depth.

Using the Mathematica<sup>TM</sup> computer package on an Apple Macintosh, models have been con-

---

Correspondence to (present address): A.C. Watkinson, An-eX, Redwood Building, King Edward VII Avenue, Cardiff CF1 3XF, U.K.

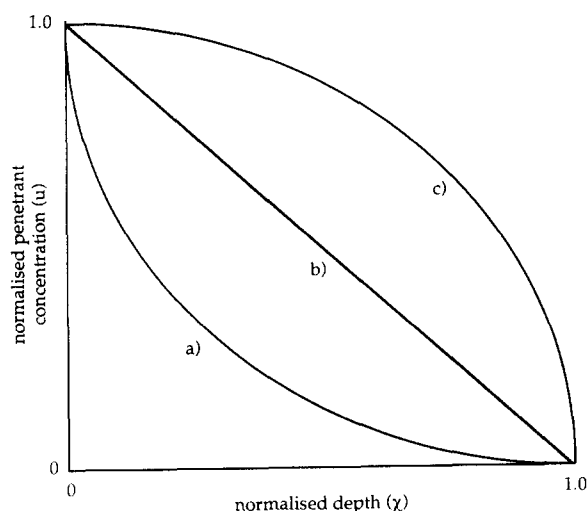


Fig. 1. (a) Example of a normalised concentration/depth profile. (b) Steady-state profile for the situation of constant diffusion coefficient. (c) Predicted steady-state profile for the situation of depth-dependent diffusion coefficient.

structured to examine and contrast the following situations:

- where the diffusion coefficient is constant;
- where the diffusion coefficient decreases with depth; and
- the effect of oleic acid (OA) on the diffusion coefficient with depth.

The equations in this first part of the model are based on Eqn 1 (Hadgraft, 1979) for the prediction of normalised concentration/depth profiles;

$$u = 1 - \chi + \left[ 2/\pi \sum_{n=1}^{n=\infty} (-1)^n / n \cdot \exp(-n^2 \cdot \pi^2 \cdot \tau) \cdot \sin(n \cdot \pi \cdot (1 - \chi)) \right] \quad (1)$$

where  $u$  is the normalised concentration ( $C/C_0$ ),  $\chi$  denotes the normalised depth ( $x/l$ ) and  $\tau = Dt/l^2$ , where  $D$  diffusion coefficient ( $t$ , time;  $l$ , sc thickness). Because Eqn 1 contains within it the assumption that the diffusion coefficient is non-

variable, the values obtained for  $u$  at higher  $\tau$  values and in the regions where the profiles start to become linear at low  $\chi$  are not correct although the general trends seen in the curves are. Theoretical steady-state profiles for the situation of varying diffusion coefficient across a membrane have been calculated previously (Crank, 1975). The results indicate a concentration profile as shown in Fig. 1c. The second section of this paper deals with the calculation of the steady-state profile for the case of the diffusion coefficient varying only part-way across the membrane and uses the FTIR data presented to make this case specific to oleic acid.

## Methods and Models

### (a) Constant diffusion coefficient

The concentration/depth profiles for constant values of  $D$  were calculated using Eqn 1 above and the Mathematica™ functions shown in Appendix 1.

### (b) Depth-dependent diffusion coefficient

To model the situation where the diffusion coefficient is depth-dependent the following approach was taken. The variability in the diffusion coefficient is proportional to the variability in  $P$ , the permeability. This can, in turn, be related to the change in the value of  $\nu(\text{C-H})$ , the C-H stretching frequency of the sc lipids, by a linear relationship. Changes in water permeability ( $P$ ) across skin with increasing temperature (ranging from 22 to 90°C) and the accompanying changes ( $\nu$ ) in  $\nu(\text{C-H})$  have been measured utilizing FTIR techniques (Potts and Francoeur, 1990). These data have been used to calculate normalised (relative to the permeability at 90°C) values of permeability,  $P_{\text{norm},90}$ , and the change in  $\nu(\text{C-H})$  associated with any particular value of  $P_{\text{norm},90}$  (Table 1).

If a linear relationship is assumed between  $P_{\text{norm},90}$  and  $\nu_{90}$  it must be forced to be of the type  $P_{\text{norm},90} = b\nu_{90} + 1$  to meet the condition  $P_{\text{norm},90} = 1$  when  $\nu_{90} = 0$ . This is easily done by rearranging to the form  $(1 - P_{\text{norm},90}) = -b\nu_{90}$ , calculating  $b$  and rearranging the fit produced to

TABLE 1

Variation in permeability of human skin to water with increasing temperature and the concurrent changes in C-H stretching frequency

Temperature (°C)	Permeability (cm h <sup>-1</sup> ) (× 10 <sup>3</sup> )	$\nu(\text{C-H})$ (cm <sup>-1</sup> )	$P_{\text{norm},90}$	$\nu_{90}$
22	0.44	2849.8	0.0135	-3.5
30	1.08	2850.1	0.0333	-3.2
40	1.94	2850.2	0.0597	-3.1
50	3.92	2850.3	0.121	-3.0
60	7.55	2850.7	0.232	-2.6
70	21.1	2851.6	0.649	-1.7
80	27.8	2852.7	0.855	-0.6
90	32.5	2853.3	1.00	0.0

yield the desired equation format. Table 2 contains the values of  $(1 - P_{\text{norm},90})$  and  $-\nu_{90}$  used to produce Eqn 2. These values are plotted in Fig. 2 with a normal regression fit through them for comparison. Using this method the value of  $b$  has been calculated as 0.296 giving Eqn 2 as shown below.

$$P_{\text{norm},90} = 0.296\nu_{90} + 1.0 \quad (2)$$

It has recently been shown that the conformational order of sc lipids is depth-dependent, becoming more ordered as the skin is penetrated. This relationship has been examined (Bommanan et al., 1990) using tape stripping and FTIR measurements (again, by examining shifts in the  $\nu(\text{C-H})$  stretching frequency).

Since the change in  $P_{\text{norm},90}$  is proportional to the alteration in  $D$ , the change in lipid order, as

TABLE 2

Values used to produce the fit given in Eqn 3

$(1 - P_{\text{norm},90})$	$-\nu_{90}$
0.9865	3.5
0.9667	3.2
0.9403	3.1
0.8790	3.0
0.7680	2.6
0.3510	1.7
0.1450	0.6
0.0	0.0

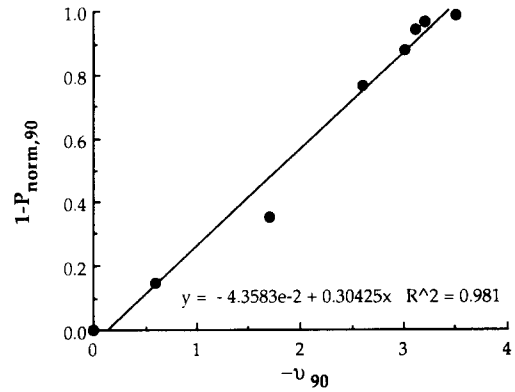


Fig. 2. Relationship between permeability and C-H stretching frequency.

indicated by  $\nu_{90}$  can be used to calculate variations in  $D$  with depth. The data from Bommanan et al. (1990) are reproduced in Table 3 along with the calculated shift ( $\nu'$ ) from  $\nu(\text{C-H})_{\chi=0}$  relative to the higher permeability measurement of  $\nu(\text{C-H})$  and the values of  $P_{\text{norm},90}$ , calculated from this shift using Eqn 2. These normalised permeabilities are therefore relative to the most permeable region of the skin, i.e., the outside layer and hence can be expressed as  $P/P_{\chi=0}$ . The corresponding values of  $\chi$  were calculated using the conclusion reached in the same paper that the amount of sc removed per tape strip remains constant at  $20 \pm 5 \mu\text{g cm}^{-2}$ . Assuming that the cumulative weight removed is propor-

TABLE 3

Variation of C-H stretch frequency with depth and its effect on permeability

Tape strip no.	$\nu'$	$P/P_{\chi=0}$	Cumulative weight of sc	$\chi$
0	0	1.000	0	0
1	-1.2	0.6448	20	0.077
2	-1.7	0.4968	40	0.154
3	-2.0	0.4080	60	0.231
4	-2.3	0.3192	80	0.308
5	-2.2	0.3488	100	0.385
6	-2.0	0.4080	120	0.462
8	-2.0	0.4080	140	0.538
10	-2.1	0.3780	180	0.692
12	-2.2	0.3488	220	0.846
14	-2.2	0.3488	260	1.000

tional to depth,  $\chi$  can be calculated from  $\chi = w/w_m$  (where  $w$  is the cumulative weight and  $w_m$  the maximum cumulative weight). These values are also included in Table 3.

Fig. 3 shows the variation of  $P/P_{\chi=0}$  as a function of position. This suggests an exponential decay in  $P$  with position expressed as;

$$\delta = \frac{\frac{P}{P_{\chi=0}} - \frac{P_{\min}}{P_{\chi=0}}}{1 - \frac{P_{\min}}{P_{\chi=0}}} = \exp(-\psi\chi) \quad (3)$$

where  $P_{\min}/P_{\chi=0} = 0.371$  and is the average value of the minimum reached by the function plotted in Fig. 3.

By plotting  $\ln \delta$  vs  $\chi$  the value of  $\psi$  was found to be 11.6. Hence, rearranging Eqn 3 and substituting for  $\psi$  gives,

$$P = P_{\chi=0}(0.629 \exp[-11.6\chi] + 0.371) \\ = P_{\chi=0} \cdot f(\chi) \quad (4)$$

Because  $P$  is proportional to  $D$  and  $\tau = Dt/l^2$  it is now possible to model variation in  $D$  with depth by altering  $\tau$  in Eqn 1

$$\tau = \tau_{\chi=0} \cdot f(\chi) \quad (5)$$

Hence, by inserting  $\tau_{\chi=0} \cdot f(\chi)$  into Eqn 1, the variation of  $D$  with depth can be approximately

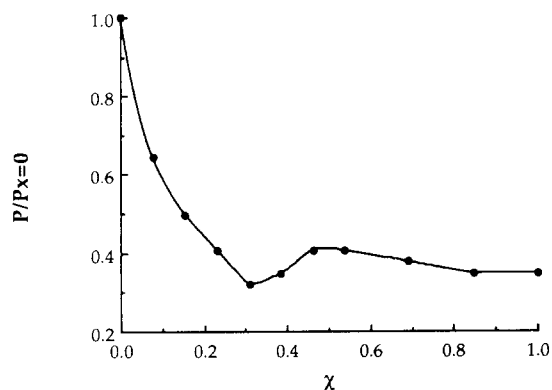


Fig. 3. Exponential type variation of permeability with depth.

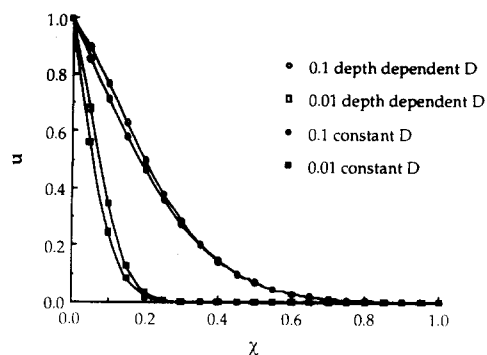


Fig. 4. Comparison, at  $\tau = 0.01$  and  $0.1$ , of diffusion profiles for depth-dependent and constant diffusion coefficient.

modelled for any original value of  $\tau$  using the Mathematica program shown in Appendix 1.

To compare these profiles with those generated for the case of a constant diffusion coefficient, the latter must be scaled accordingly. This is achieved by premultiplying  $\tau$  by  $0.371$  in Eqn 1 in the case of constant  $D$ . This allows the two profiles to be compared as the minimum values of  $D$  in the depth-dependent case should be equal to the constant value where  $D$  is non-variable. Fig. 4 compares the situations of constant and variable diffusion coefficients for values of  $\tau_{\chi=0} = 0.01$  and  $0.1$ . The plots demonstrate how the initial disorder of skin lipids at low  $\chi$  affects the theoretical diffusion profile of a drug. As can be seen from these graphs there is very little difference between those produced with a depth-dependent diffusion coefficient and those generated with a constant value of  $D$ .

### (c) Calculation of profiles at steady state after oleic acid treatment

Using tape stripping techniques and FTIR measurements in a similar manner to those quoted above, the effect of oleic acid on sc lipid order has been monitored as a function of depth (Naik, 1990; Guy et al, 1992). The modelling described in the previous section was unable to predict the steady-state profile shape for an analogous situation because of the limitations inherent in the model used. In this section the effect of oleic acid on the steady-state diffusion profile will be predicted by a numerical method.

TABLE 4

Permeability and C-H stretch data normalised to the low temperature values

$P_{\text{norm},22}$	(C-H) shift relative to that at 22°C
1.00	0
2.46	0.3
4.41	0.4
8.91	0.5
17.16	0.9
47.96	1.8
63.18	2.9
73.86	3.5

These data (Naik, 1990) were expressed relative to the low permeability value for  $\nu(\text{C-H})$ , meaning the initial 'calibration plot' (Fig. 2) must be adjusted to make it of use in the interpretation of these results. By normalising the  $\nu$  (the shift in wavenumber) and  $P$  values in Table 1 relative to the low permeability figures, the data in Table 4 are produced. A similar fit to this data can be carried out as in the preceding section, producing Eqn 6 for the relationship between  $P_{\text{norm},22}$  and  $\nu_{22}$ .

$$P_{\text{norm},22} = 21.43\nu_{22} = 1.0 \quad (6)$$

Eqn 6 can now be used to calculate values of  $P_{\text{norm},22}$  from the shift that occurs in the presence of oleic acid. The relevant values of  $\chi$  were calculated from data collected by the same workers (Naik, 1990) using the assumptions and methods as in the previous section. These data are listed in Table 5.

As stated in the Introduction, the concentration/depth profile at steady-state will probably be curved above that predicted by the methods used above. The equations below (see Appendix 2) describe exactly what the shape of this profile will be in the case of oleic acid changing the diffusion coefficient with depth.

(i) where,

$$0 \leq \chi < \chi^*$$

TABLE 5

Variation of C-H stretch frequency on treatment with OA and the calculated accompanying change in permeability

(C-H) shift in the presence of OA	$P_{\text{norm},22}$	Tape strip no.	$\chi$
5.0	108.15	0	0
2.6	56.72	1	0.197
1.3	28.86	2	0.326
0.2	5.286	3	0.471
0.0	1.000	4	0.581

we obtain,

$$u = C/C_0 = 1 - \left( \frac{\frac{1}{b} \ln \left( \frac{a}{a - b\chi} \right)}{\frac{1}{b} \ln(a) + L - \chi^*} \right) \quad (7)$$

(ii) where,

$$\chi^* < \chi \leq L$$

we obtain,

$$u = C/C_0 = \left( \frac{\frac{1}{b} \ln(a) + L - \chi}{\frac{1}{b} \ln(a) + L - \chi^*} \right) \quad (8)$$

where  $C$  is the drug concentration (mass per unit volume) in a differential element at axial position  $\chi$ ,  $C_0$  denotes the surface drug concentration,  $\chi$

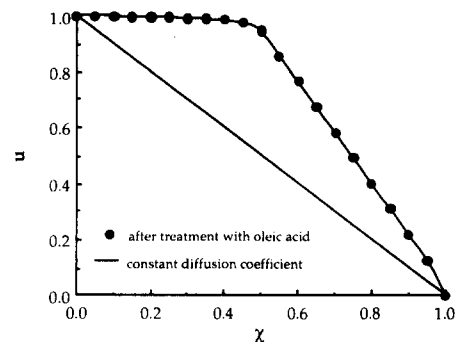


Fig. 5. Simulated effect of oleic acid on the diffusion profile at steady state.

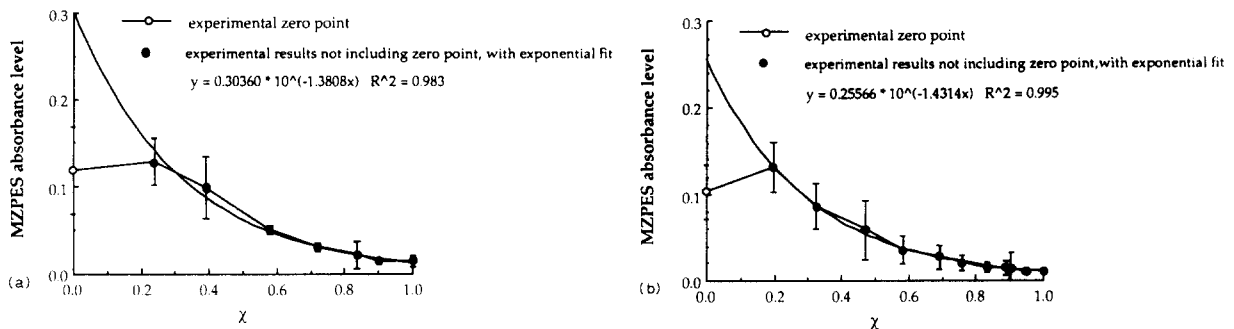


Fig. 6. (a) Comparison of exponentially fitted experimental data (2 h) with the same data including the previously ignored zero point (b) Comparison of exponentially fitted experimental data (3 h) with the same data including the previously ignored zero point.

is the normalised axial position (depth) of the differential element,  $t$  represents time and  $L = 1$ .

For the case of oleic acid the values of  $a$ ,  $b$  and  $\chi^*$  have been evaluated by carrying out a linear fit to the data shown in Table 5. Linear regression yields  $a = 104.4$ ,  $b = 220.0$ ,  $\chi^* = 0.471$  ( $r^2 = 0.99$ ). Using these values in Eqns 7 and 8 and the Mathematica program in Appendix 1(iii), the steady-state profile of normalised drug concentration vs normalised depth was calculated and is depicted in Fig. 5.

## Discussion

The efficacy of this type of approach can be demonstrated by comparing the calculated profiles with those obtained experimentally by other workers. The effect of OA on the concentration-depth profile of a model antifolate used in the treatment of psoriasis (*m*-azidopyrimethamine ethanesulphonate or MZPES) has been investigated in vivo by FTIR techniques (Naik, 1991). In this work,  $\log[\text{drug concentration}]$  vs depth penetrated into the sc was found to be linear at 1, 2 and 3 h. However, in the initial analysis, the first data points at 'zero' depth from these plots were omitted because they fell well below the exponentially fitted line. It was assumed that surface washing had lowered the first layer's drug content. The low values of these omitted data points can be accounted for by the shape of the calculated concentration-depth profile for OA-treated

skin, i.e., the shape of the calculated curve in Fig. 5 is very similar to those that include all the data points depicted in Fig. 6a and b. Since there is little difference between the 2 and 3 h graph diffusion could also have reached steady state. It can be seen that it is quite possible that the relatively low values of concentration at  $\chi = 0$  can be accounted for by this profile shape.

Hence, it is possible that the correct shape for these normalised plots is as predicted by the theoretical steady-state curve and that a logarithmic fit to this type of data is incorrect.

## Conclusions

The rapid calculation of approximate normalised concentration-depth profiles has been achieved by computer simulation. The model can be used to predict the general shapes of concentration/depth profiles and has qualitatively demonstrated how the natural non-uniformity of the sc lipid packing may not affect these types of profiles.

The calculation of the steady-state profile for the case of the diffusion coefficient varying only part-way across the membrane has been carried out using FTIR data to make this case specific to oleic acid. It has also been demonstrated that it is not necessarily correct to assume a logarithmic type fit to concentration-depth data collected from tape strip experiments.

## Appendix 1

*Mathematica*<sup>TM</sup> programs for the simulation of concentration / depth profiles

(i) Values of  $u$  for the non-variable  $D$  case were calculated using:

```
u=Flatten[Table[{x,1-x
+(2/Pi*Sum[(((1/n)^n)/n)
*Exp[-(n^2)*(Pi^2)*t]
*Sin[Pi*n*(1-x)]},
{n,1,10}]]],{x,0,1,0.05}],1]
```

where  $x = \chi$  and  $n$  ranges from 0 to 10. This instruction produces a table of values of  $u$  and  $x$  from a generated list of  $x$  ranging from 0 to 1.0 at intervals of 0.05, i.e., of the form  $\{x_1, x_2, x_3, x_4, \dots, u_1, u_2, u_3, u_4, \dots\}$ . The list must then be partitioned into numerical pairs of the form  $\{\{x_1, u_1\}, \{x_2, u_2\}, \dots\}$  and then plotted. This is achieved by the following instructions:

```
Partition [u,2]
q=N[%]
b=ListPlot [q,PlotJoined->True]
```

(ii) Values of  $u$  for the variable  $D$  case were calculated using:

```
u=Flatten[Table[{x,1-x
+(2/Pi*Sum[(((1/n)^n)/n)
*Exp[-(n^2)*(Pi^2)*t]
*(.629*Exp[-11.6x]+.371)]
*Sin[Pi*n*(1-x)]},{n,1,10}]]],
{x,0,0.4,0.05}],1]
```

The above instruction produces a list in a similar fashion to that in (i). The following instructions produce the result,

```
w=N[%]
y=Partition[w,2]
ListPlot[y,PlotJoined->True]
```

(iii) The steady-state solution for variable diffusion coefficient was calculated as follows:

Firstly the values of the constants are defined, i.e., the depth to and the rate at which the diffusion coefficient varies,

$a = 104.4$ ,  $b = 220$ ,  $L = 1$ ,  $w = 0.471$  (where  $w = \chi^*$ ).

```
u=Table[{x,1-(((1/b)*Log[a/(a-
(b*x))])/(((1/b)*Log[a]+L-w)))},
{x,0,0.45,0.05}]
p=Table[{x,(((1/b)*Log[a]+1-x))
/(((1/b)*Log[a]+L-w)}},
{x,0.5,1,0.05}]
q=Join[u,p]
ListPlot[q,PlotJoined->True]
```

This program allows the extent and magnitude of the variation in  $D$  to be changed (by simply altering the values of  $a$ ,  $b$ ,  $L$  and  $w$ ) as long as the fit to the variation is linear.

## Appendix 2

*Derivation of the concentration / depth profile at steady state*

If,  $C$  represents the drug concentration (mass per unit volume) in a differential element at axial position  $x$ ,  $x$  is the axial position (depth) of the differential element and  $t$  denotes time, then,

$$\frac{\partial C}{\partial t} = \frac{\partial N}{\partial x} \quad (\text{A1})$$

where  $\partial C / \partial t$  represents the rate of accumulation of drug in a differential element and  $\partial N / \partial x$  is the flux of drug in and out of a differential element, where  $N$  denotes the flux of drug across a stationary area which, from Fick's first law, is given by,

$$N = -D \cdot \frac{\partial C}{\partial x} \quad (\text{A2})$$

where  $D$  is the diffusion coefficient. Thus,

$$\frac{\partial C}{\partial t} = \frac{\partial N}{\partial x} = -\frac{\partial}{\partial x} \left( D \cdot \frac{\partial C}{\partial x} \right) \quad (\text{A3})$$

Note that if the diffusion coefficient,  $D$ , is a function of normalised depth,  $\chi$ , then;

$$\frac{\partial}{\partial \chi} \left( D \cdot \frac{\partial C}{\partial \chi} \right) \neq D \cdot \frac{\partial^2 C}{\partial^2 \chi}$$

where  $\chi$  denotes the normalised depth ( $x/l$ ). At steady state;

$$\frac{d}{d\chi} \left( D \cdot \frac{dC}{d\chi} \right) = 0 \quad (\text{A4})$$

Integrating Eqn A4 twice yields,

$$C = C_0 \cdot \left( 1 - \frac{\int_0^\chi \frac{d\chi}{D(\chi)}}{\int_0^L \frac{d\chi}{D(\chi)}} \right) \quad (\text{A5})$$

To proceed further, the variation in  $D$  must be given a mathematical form. If the function  $D(\chi)$  is expressed as a linear variation ( $D(\chi) = D_0 \cdot (a - b\chi)$ ) up to a depth  $\chi^*$  and then from  $\chi^*$  to  $L$  as zero variation ( $D(\chi) = D_0$ ), the following conditions apply (note that these conditions mean that  $a - b\chi^* = 1$ ),

$$\frac{D}{D_0} = a - b\chi \quad \text{at } 0 \leq \chi < \chi^*$$

$$\frac{D}{D_0} = 1 \quad \text{at } \chi^* \leq \chi \leq L$$

Placing these conditions into Eqn A5 yields Eqns 7 and 8 shown in the main text.

## References

- Bommannan, D., Potts, R.O. and Guy, R.H., Examination of the stratum corneum barrier function in vivo by infrared spectroscopy. *J. Invest. Dermatol.*, 95 (1990) 403–408.
- Crank, J., *The Mathematics of Diffusion*, Oxford University Press, Oxford, 1956, pp. 147–185.
- Guy, R.H., Higo, A., Bommannan, D., Ramanathan, V., Griffin, R., Irwin, W.J. and Potts, R.O., Mechanism of enhancement of skin penetration in vivo. In Scott, R.C., Guy, R.H., Bodde, H.E. and Hadgraft, J. (Eds), *Prediction of Percutaneous Penetration. Methods, Measurement and Modelling*, 2nd Edn, IBC Technical Services, London, 1992, pp. 1–12.
- Guy, R.H., Mak, V.H.W., Kai, T., Bommannan, D., and Potts, R., Percutaneous penetration enhancers: mode of action. In Scott, R.C., Guy, R.H. and Hadgraft, J. (Eds), *Prediction of Percutaneous Penetration*, IBC Technical Services London, 1990, pp. 213–223.
- Hadgraft, J., Calculations of drug release from controlled release devices. The slab. *Int. J. Pharm.*, 2 (1979) 177–194.
- Mak, V.H.W., Potts, R.O. and Guy, R.H., Percutaneous penetration enhancement in vivo measured by attenuated total reflectance infrared spectroscopy. *Pharm. Res.*, 7 (1990) 835–841.
- Naik, A., Azidoprofen as a soft anti-inflammatory agent for the topical treatment of psoriasis, Ph.D. Thesis, University of Aston, UK (1990).
- Potts, R.O., and Francoeur, M.L., Lipid biophysics of water loss through the skin. *Proc. Natl. Acad. Sci. USA*, 87 (1990) 1–3.